



An Investigation of Impedance Determination using Two-Point High Frequency Injection Technique for Non-Contact Voltage Measurement System

Noppawit Longseng¹, Kittikhun Thongpull^{1,*}

¹ Department of Electrical Engineering, Faculty of Engineering, Prince of Songkla University, Kohong, Hat-Yai, Songkhla 90110, Thailand

ARTICLE INFO

Article history:

Received 2 January 2024

Received in revised form 17 June 2024

Accepted 21 August 2024

Available online 19 September 2024

Keywords:

Capacitive coupling; high frequency injection; non-contact voltage measurement

ABSTRACT

Energy management facilities are becoming more necessary due to the growth of smart energy and microgrid technologies. Convenient access to information on energy consumption is an advantage for energy planning and management and secure for the operators. Consequently, these conceive the idea of developing non-contact sensor approach to replace the conventional energy measurement while maintain full accessibility to voltage and current information. This paper proposes a method of non-contact conductive voltage measurement with an automated calibration system. The previous application of non-contact voltage measurement systems in the low-voltage range used a method based on the capacitive coupling principle by covering a metal plate around an insulated power line cable. The important factor of measurement accuracy depends on the determination of impedance occurring between the conductors within the cable and the metal plates attached to the cable surface by insulating as a dielectric. The proposed impedance determination process employs a two-point high-frequency signal injection technique that transmits a reference signal to calculate the established parasitic impedance value. From the high-frequency injection technique, the resulting impedance can be calibrated throughout the reverse calculation to measure the actual voltage of the power line. The experimental results of the proposed voltage measurement system can measure the actual voltage of the power line with the capability to calibrate the impedance due to the variation in the environment and eliminate noise errors from the instability under various conditions.

1. Introduction

The development of sensors for non-contact voltage measurement has gained attention for monitoring electricity distribution systems due to its advantages in terms of convenience and safety. Several approaches can be used to realize a non-contact voltage sensor, such as taking advantage of parasitic capacitance [1] or using the near-field detection principle [2]. The most popular technique is the principle of electric field coupling, which forms a coupling capacitance from two conductive

* Corresponding author.

E-mail address: kittikhun.t@psu.ac.th

<https://doi.org/10.37934/araset.51.2.215226>

with an insulator acting as a dielectric layer to be used as a sensor. Several research schemes present a review of different capacitor values, such as obtained capacitance from the cylindrical capacitor [3-5], and obtained capacitance from switching circuits [6,7], taking advantage of two-frequency circuit analysis [8].

The capacitance value is vital information of capacitive coupling methods and should be accurately determined. In advance, based on Shenil and George [9-12] author studied factors that affect voltage measurements, such as considering the position between the conductors within the cable and electrode [9], considering harmonics that affect the calculated voltage value [10], considering the impedance changes that occur between grounding and power circuits [11] and other possible capacitances among electrode [12]. In addition, the improvement of signal accuracy despite electromagnetic disturbance is reported in [13]. A study of the capacitance that forms at high voltage levels is presented in [14]. A probe set was designed for use in low-voltage cables [15] and for high-voltage cables [16]. The relationship between the voltage measured from the sensor and voltage in cables from articles is studied in [17,18]. Monitoring of high-voltage voltage in transmission lines in distribution systems was conducted in [19,20]. Furthermore, the development of wireless overvoltage detection has been experimented in [21].

One of the main challenges with non-contact voltage measurement approaches is determining the consist of the sensor. Previous schemes have shown that efforts have been made to consider the effects on sensors and measurement systems of both environmental and technical restrictions. Previous methods have neglected the potential components of parasitic capacitance between the sensor and the signal cable connection or the front-end circuit. This paper presents impedance estimation using the proposed two-point high-frequency injection technique. The proposed technique can determine the impedance among the elements used as sensor electrodes. Impedance values can be calibrated according to environmental changes or sensor probe degradation with the proposed technique. Thus, the obtained impedance value can be used to calculate the actual capacitance value and achieve accurate voltage measurement. The experimental results and applications of the developed technique are described in the following sections.

2. Methodology

2.1 Theories and Principles

The characteristics of the sensor are designed according to the principle of capacitive coupling. A copper sheet is used as a measurement electrode wrapped around the surface of a powerline cable at a length $l = 3cm.$, causing the copper sheet to form a cylindrical capacitor between the conductor inside the cable with radius R_1 and the external electrode of the R_2 separated by the insulation material with dielectric of ϵ . The formed capacitance can be calculated using the equation mentioned in [5] below.

$$C = \frac{2\pi l \epsilon}{\ln \frac{R_1}{R_2}} \quad (1)$$

The capacitors obtained from this process are exploited as electrical connection terminals as shown in Figure 1. However, utilizing the electrode as a sensor requires the knowledge of the capacitance value while operating despite using a fixed value for voltage calculation. Temperature changes, humidity, and the surrounding environment significantly cause the sensor to deteriorate which results in variations in the physical properties of the cable insulation. Thus, the permittivity (ϵ)

value as well as the capacitance are subject to drift and ultimately error in voltage measurement as has been mentioned in [22]. Furthermore, the two sensor electrodes on the cable also have a parasitic resistance between each other affecting the total impedance of the sensor.

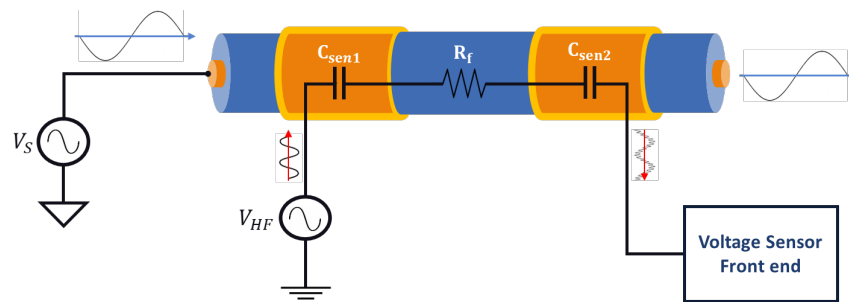


Fig. 1. Characteristics of cylindrical capacitor applied as a sensor

2.2 Two-Point High Frequency Injection Technique

From the characteristics of the proposed measurement concept, it has both a receiver for measuring output signal and a transmitter for injecting high-frequency signal into the cables as shown in Figure 1. The impedance between the two sensor terminals can be explained as a series of resistance R_f and capacitance C_{sensor} , as shown in Figure 2. The analogue front-end circuit is designed as a resistor relative to the capacitance of the sensor as a passive high-pass filter circuit relationship between the C_{sensor} and the R_{HP} . However, from considering the impedance value of the sensor to correctly calculate the C_{sensor} and R_f values, it is necessary to consider the impedance factor of the device used to measure the signal $Z_{measurement}$. This impedance is separated into the input impedance of the probe and the oscilloscope as shown in Figure 2. The equation for the impedance relationship of the measuring device is as follows.

$$Z_{S\&P} = \frac{\omega(R_p C_p + R_{SC} C_p) - j}{\omega(C_{SC} + C_p) + j\omega^2 C_p C_{SC} (R_p + R_{SC})} \quad (2)$$

From Eq. (2), the impedance fraction of the measuring device can be divided as follows: $Z = \frac{A}{B}$. Can be separated to $A = \omega(R_p C_p + R_{SC} C_p) - j$ and $B = \omega(C_{SC} + C_p) + j\omega^2 C_p C_{SC} (R_p + R_{SC})$. The impedance on the front-end circuit will be obtained as follows.

$$Z_{S\&P} = \frac{R_{HP} \cdot A}{R_{HP} \cdot B + A} \quad (3)$$

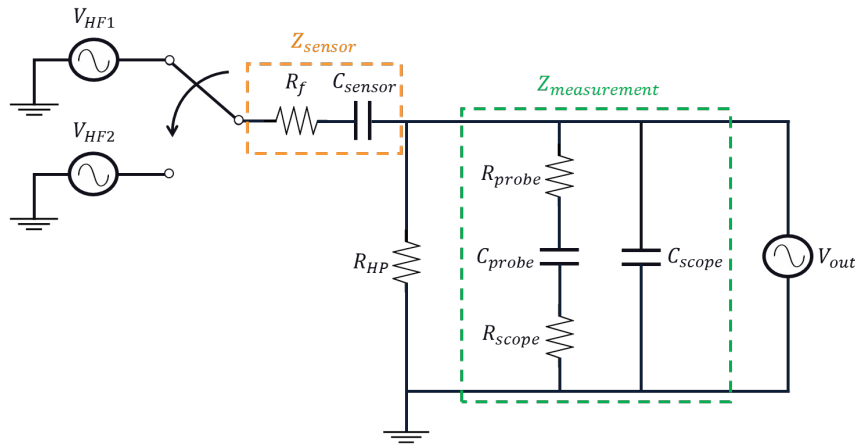


Fig. 2. Simulated circuit for measuring resistance and capacitance applying a two-point high-frequency injection technique

When a high-frequency signal is injected into the sensor and the signal is measured and compared with the signal on the receiver side, V_{out} will be obtained as shown in Figure 3. Obviously, the F_{out} signal receiving point frequency equal to the F_{HF} signal injection point frequency, and the output waveform is attenuated together with the phase shift that occurs as a result of the impedance within the system. It's considered a concept of the technique of injecting two-point high frequencies into the system to analyse two frequencies in circuits with the same components. The technique is injecting two high frequencies into the system and comparing the amplitude and phase shift angles of the sensor's output and input signals. It can be analysed as the result of two equations with two frequencies as follows.

$$V_{out1} = \frac{A_1 \cdot j\omega_1 C_{sensor} R_{HP}}{A_1 \cdot j\omega_1 C_{sensor} R_{HP} + (B_1 \cdot R_{HP} + A_1)(1 + j\omega_1 C_{sensor} R_f)} V_{HF1} \quad (4)$$

$$V_{out2} = \frac{A_2 \cdot j\omega_2 C_{sensor} R_{HP}}{A_2 \cdot j\omega_2 C_{sensor} R_{HP} + (B_2 \cdot R_{HP} + A_2)(1 + j\omega_2 C_{sensor} R_f)} V_{HF2} \quad (5)$$

Eq. (4) and Eq. (5) can be reformulated to find the desired impedance value by replacing X and Y with R_f and $\frac{1}{C_{sensor}}$ respectively. The form of two equations with two variables will be obtained as follows.

$$V_{out1} \cdot j\omega_1 (B_1 \cdot R_{HP} + A_1) X + V_{out1} \cdot (B_1 R_{HP} + A_1) Y = (V_{HF1} - V_{out1}) A_1 \cdot j\omega_1 R_{HP} \quad (6)$$

$$V_{out2} \cdot j\omega_2 (B_2 \cdot R_{HP} + A_2) X + V_{out2} \cdot (B_2 R_{HP} + A_2) Y = (V_{HF2} - V_{out2}) A_2 \cdot j\omega_2 R_{HP} \quad (7)$$

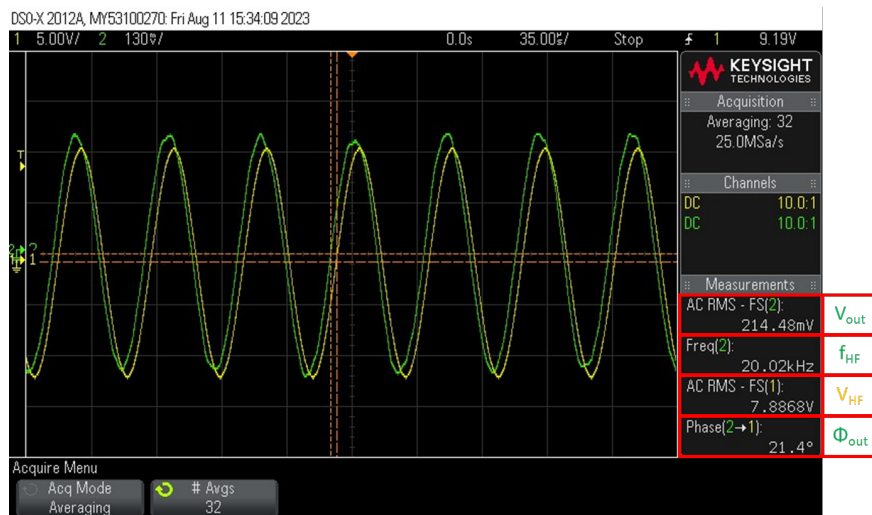


Fig. 3. The signal at the receiving point is compared to the signal injected into the sensor

3. Results

Preliminary experiment at room temperature 25°C as shown in Figure 4. The sensor impedance compared to humidity change in the surrounding area of the sensor.

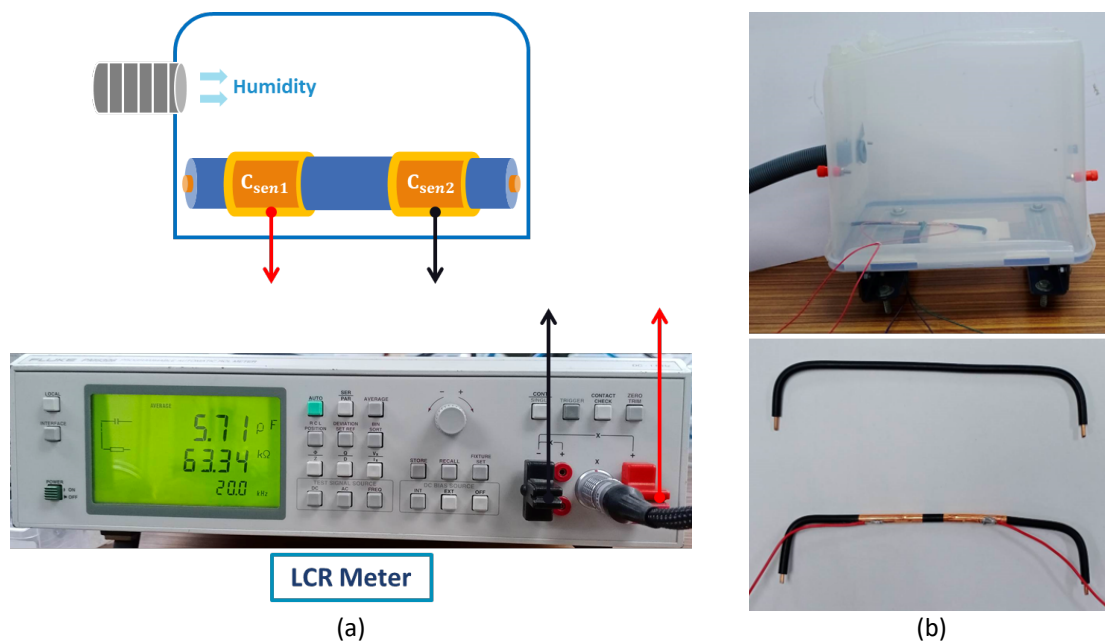


Fig. 4. Experiment to measure capacitance and resistance versus humidity (a) Set up the experimental equipment (b) Example of the sensor and preparation of the preliminary box

The experimental results depicted as plots in Figure 5 shown that capacitance and resistance increase with increasing humidity, with a significant effect in the case of humidity greater than 80% RH at 25°C. In the worst-case scenario, capacitance changed by 1.75% and resistance changes by 11.92% at 90% RH at 25°C humidity, compared to the humidity at 50% RH at 25°C. Based on the problem, this paper proposes a method to determine the resistance and capacitance using a two-point high-frequency injection technique into the transmit terminal of the sensor. Consider the signal

output and compare it with the input signals for calibrating the impedance between two sensor terminals within the circuit before calculating the voltage in the cable.

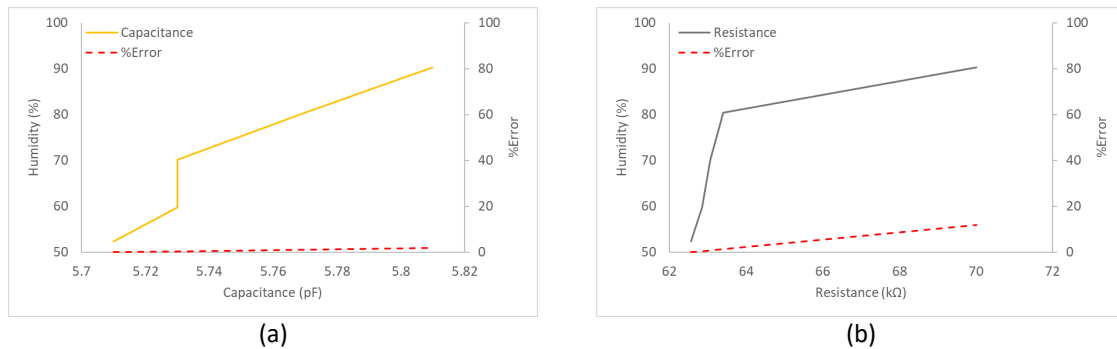


Fig. 5. Plots of comparing capacitance and resistance measurement results with humidity (a) Plot of change in capacitance value compared with humidity (b) Plot of change in resistance value compared with humidity

A preliminary experiment to test the accuracy of the resistance and capacitance measurement technique from Eq. (6) and Eq. (7) is shown in Figure 6. The test circuit includes passive components resistors in a range of 10kΩ - 500kΩ, and capacitors in the 10pF - 100pF.

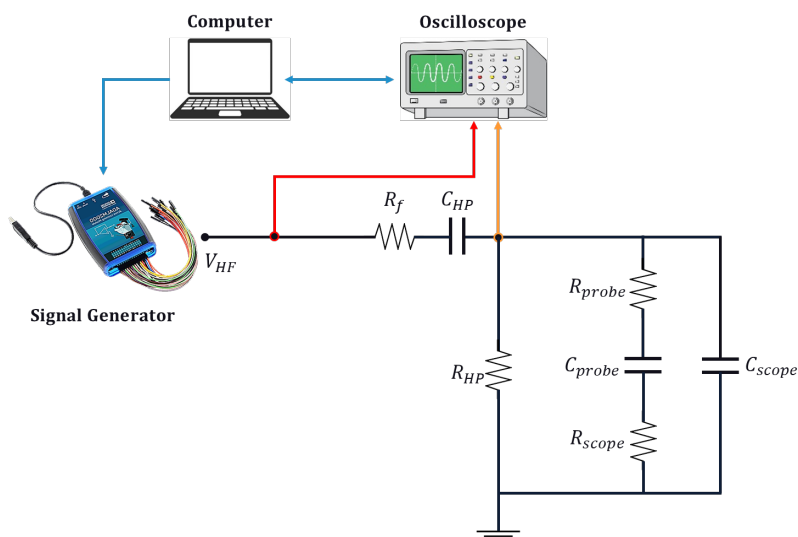


Fig. 6. Set up of preliminary experiment of the two-point high-frequency injection technique

The first experiment measures the impedance value by changing resistors from 10kΩ - 500kΩ and has trial parameters as shown in Table 1. Compare the impedance value from the two-point high-frequency injection technique with the impedance measured by the FLUKE PM6306 RCL meter. The procedure for each impedance measurement is a total of 10 two-point high-frequency measurements. A total of 5 values for each of the resistors and capacitors will be obtained by Eq. (6) and Eq. (7).

Table 1
 Parameter components of the preliminary experiment

Components	Value
C_{sensor}	100 pF
R_{HP}	300 k Ω
R_{probe}	10 M Ω
C_{probe}	15 pF
R_{scope}	1 M Ω
C_{scope}	15 pF
F_{HF1}	10 kHz
F_{HF2}	20 kHz

The five values are averaged to $R_{f_cal_avg}$ and $C_{\text{HP_cal_avg}}$ before being compared with the results of measuring the resistor R_{f_real} and capacitor $C_{\text{HP_real}}$ with the RCL meter. This procedure was to confirm the repeatability of the measurement of both elements in the experiment. The results of the impedance measurement experiment by changing the resistor are shown in Table 2.

Table 2
 Impedance measurement results by modifying the resistor

Resistor (k Ω)	R_{f_real} (k Ω)	$R_{f_cal_avg}$ (k Ω)	%Error $_{R_f}$	$C_{\text{HP_real}}$ (pF)	$C_{\text{HP_cal_avg}}$ (pF)	%Error $_{C_{\text{HP}}}$
10	9.9511	9.6538	4.8764	99.36	102.68	3.3368
12	11.916	12.275	4.6752	99.36	101.88	2.5331
15	14.720	14.028	4.7031	99.36	102.07	2.7245
18	17.677	17.492	3.6139	99.36	101.78	2.4325
20	19.716	19.870	2.1080	99.36	101.67	2.3220
22	21.703	21.708	4.7461	99.36	101.80	2.4539
24	23.909	24.426	3.7261	99.36	101.30	1.9550
27	26.536	25.981	4.5658	99.36	101.52	2.1760
30	30.126	30.021	0.8173	99.36	101.06	1.7104
39	38.289	37.318	2.5348	99.36	100.84	1.4944
47	47.418	46.642	1.8083	99.36	101.89	2.5413
51	50.515	50.147	0.9194	99.36	101.34	1.9913
56	55.507	54.928	1.0438	99.36	100.50	1.1485
68	67.943	67.272	0.9882	99.36	102.09	2.7504
75	73.759	71.271	3.3726	99.36	103.45	4.1158
82	81.135	80.268	1.0688	99.36	102.01	2.6638
100	99.497	98.395	1.1080	99.36	101.63	2.2827
120	119.63	118.77	0.7202	99.36	102.20	2.8537
180	176.17	175.86	0.2697	99.36	102.82	3.4840
220	221.31	221.61	0.2329	99.36	103.57	4.2373
240	236.61	236.15	0.2459	99.36	105.79	6.4720
300	300.61	309.89	3.0884	99.36	103.62	4.2884
330	327.13	338.10	3.3538	99.36	103.69	4.3529
390	387.84	401.79	3.5959	99.36	107.81	8.5009
470	467.82	496.96	6.2299	99.36	105.15	5.8246
500	506.66	538.99	6.3807	99.36	104.48	5.1563

The second experiment measures the impedance value by changing the capacitor from 10pF – 100pF and having the same parameters components as Table 3 but changing from C_{sensor} to R_f equal to 300k Ω . The procedure is the same as the first experiment, but only changing the capacitor. The results of the impedance measurement experiment by changing the resistor are shown in Table 3.

Table 3
 Impedance measurement results by modifying the capacitor

Capacitor (pF)	C_{HP_real} (pF)	$C_{HP_cal_avg}$ (pF)	%Error $_{C_HP}$	R_{f_real} (k Ω)	$R_{f_cal_avg}$ (k Ω)	%Error $_{R_f}$
10	10.25	9.9289	3.1328	300.59k	307.85	2.4157
12	12.49	12.15	2.7189	300.59k	303.83	1.0772
22	22.01	22.658	2.9431	300.59k	307.29	2.2302
27	27.24	29.01	5.3390	300.59k	305.58	1.6588
33	33.06	34.409	4.0813	300.59k	306.12	1.8388
39	40.18	42.291	5.2540	300.59k	311.48	3.6219
47	47.15	48.337	2.5182	300.59k	310.04	3.1444
56	59.96	62.119	3.6012	300.59k	310.74	3.3758
68	65.81	68.173	3.5907	300.59k	310.11	3.1675
100	100.72	103.91	3.1711	300.59k	309.25	2.8813

The experimental setup for measuring voltage in the cable is shown in Figure 7. The cable used is a THW cable, size 4 sq.mm. installed sensor with a copper sheet as an electrode, length 3 cm. 2 terminals separate distance 1 cm. A computer control unit controls the injection of high frequency to sensors and switches by supplying logic unit voltage through a signal generator. After the frequency is applied to the sensor, the resistance R_f and capacitance C_{sensor} can be calculated with Eq. (6) and Eq. (7). The control unit then switches SW_1 to disconnect the high-frequency signal to measure the voltage drop across R_{HP} in the fundamental frequency from the V_S supply. V_{out} is calculated as the line voltage by converting Eq. (4) or Eq. (5) by replacing V_{HF} with V_{out} and calculating the remaining variables at the same frequency as V_{out} . The voltage in the cable can be obtained by the following equation.

$$V_S = \frac{A_S \cdot j\omega_S C_{sensor} R_{HP} + (B_S \cdot R_{HP} + A_S)(1 + j\omega_S C_{sensor} R_f)}{A_S \cdot j\omega_S C_{sensor} R_{HP}} V_{out} \quad (8)$$

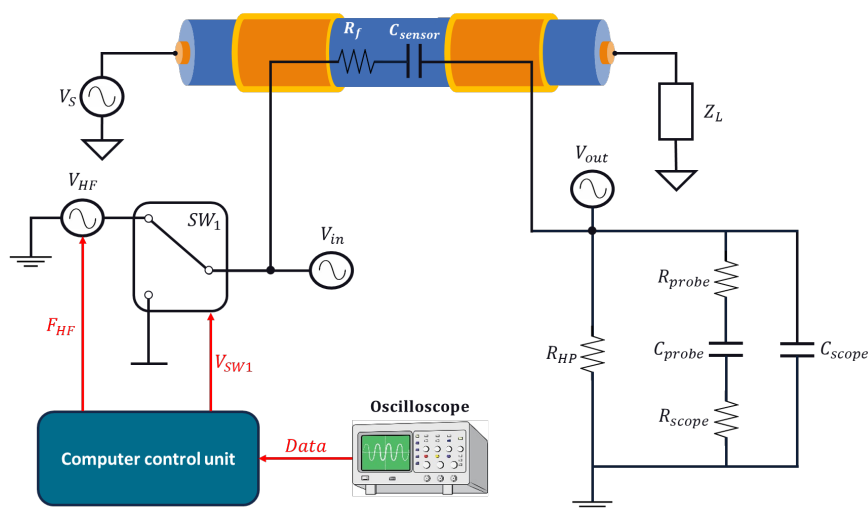


Fig. 7. Experiment setup of non-contact voltage measurement by high-frequency injection technique

The voltage measurement experiment was tested with 3 types of loads: a light bulb, a kettle, and a capsule coffee maker, as shown in Figure 8.

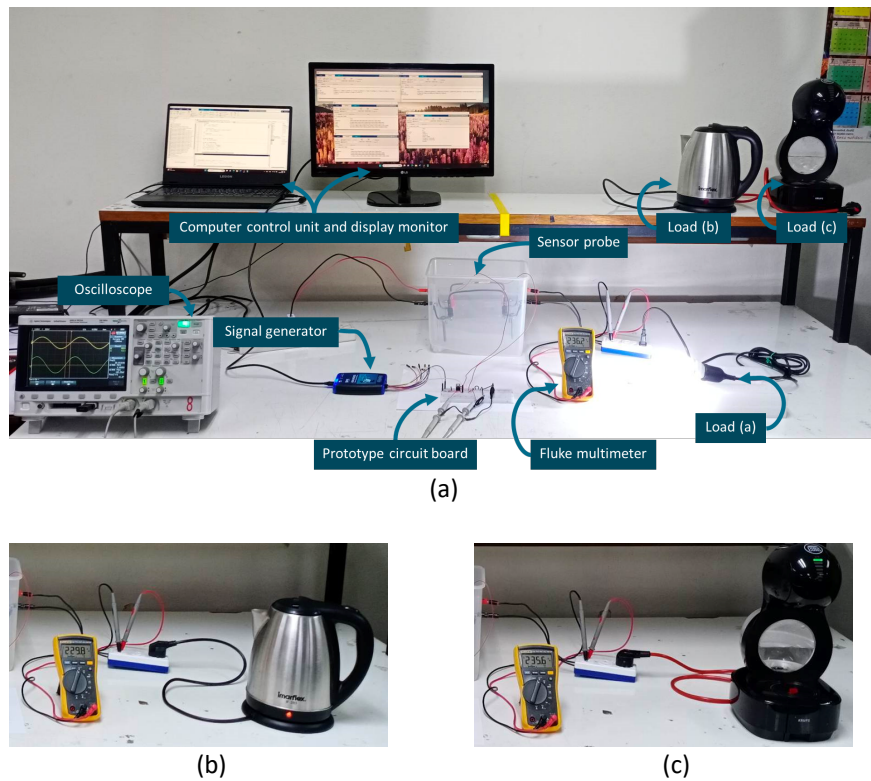


Fig. 8. Experiment setup for 3 types of loads (a) light bulb (b) kettle (c) capsule coffee maker

The voltage measurement results are shown in Table 4, with the same parameters component as Table 1, only replacing C_{sensor} and R_f with the values calculated from Eq. (6) and Eq. (7). Voltage measurement experiment, each test load was measured 10 times in total to find the average value of the source voltage $V_{S_real_avg}$ and the average value of the calculated voltage $V_{S_cal_avg}$ with Eq. (8). The calculated voltage values were compared with the measured voltage values from the FLUKE 115 multimeter.

Table 4

Voltage was measured by a two-point high-frequency injection technique

Load	$V_{S_real_avg}$ (V)	$V_{S_cal_avg}$ (V)	%Error v_{S_avg}	$C_{sensor_cal_avg}$ (pF)	$R_f_cal_avg$ (k Ω)
Light bulb	236.23	232.53928	1.5622	12.7992	370.208
Electric kettle	230.18	230.84524	0.3097	12.8502	368.636
Coffee maker	235.68	232.94817	1.1591	12.8796	368.205

The non-contact voltage measurement techniques of each scheme in each research were compared as presented in Table 5. Techniques in each of the previous schemes only considered the coupling capacitance from the sensor, as reported in [4,5]. Recently techniques were developed that led to consideration of both the coupling capacitance formed by the sensor and the parasitic capacitance periphery as reported in [9,10,16]. This proposed scheme presents a consideration of the impedance of a sensor, which consists of a coupling capacitance and a resistance. Considering components other than capacitance due to electric field coupling, determining the impedance in the sensor probe is important for calculating the voltage in the cable. The main advantage of the two-point high-frequency injection technique is impedance measurement because the technique can calculate the sensor impedance on any sensor probe from Eq. (6) and Eq. (7). The flexibility provided

by the proposed technique reduces the complexity of determining parasitic capacitance for calibration and reverse calculation of voltages in the cable.

Table 5
 Comparison of measurement methods in different techniques

Comparison topic	[4]	[5]	[9]	[10]	[16]	This Work
Measurement computations	Capacitive voltage divider	Switching filters circuit	Dual slope conversion	FFT magnitude and phase	Capacitive voltage divider	Two-Point High Frequency
Principle used	Electric field coupling	Electric field coupling	Electric field coupling	Electric field coupling	Electric field coupling	Electric field coupling
Probe considering	C_{sensor}	C_{sensor}	$*C_{\text{sensor}}$	$*C_{\text{sensor}}$	$*C_{\text{sensor}}$	$C_{\text{sensor}}, R_{\text{sensor}}$
Maximum range	220 V	230 V	400 V	600 V	\blacklozenge 40 kV	230 V
Frequency	50 Hz	50 Hz	50-60 Hz	50-60 Hz	50 Hz	50 Hz
Accuracy	2.5%	<3%	0.26%	0.31%	<5%	<2%

*-Consider parasitic capacitances or stray capacitances around the sensor probe, \blacklozenge -High voltage measurement

4. Conclusions

The proposed two-point high-frequency injection technique for noncontact voltage sensor is developed to estimate the impedance. The proposed technique has the advantage of being able to measure more than one internal component. Another advantage of its use is that it can be injected into two terminals between the elements to be measured without intrusive on the intermediary, in this case, the conductors within the cable. The accuracy of the technique is shown as the preliminary experimental results by measuring a resistor in series with a capacitor by adjusting the resistors as 2.7228% and 3.3001% respectively. The accuracy of impedance measurement by adjusting capacitors were 2.5412% and 3.6350%, respectively. From these results, the two-point high-frequency injection technique can achieve acceptable accuracy of impedance values.

The application of the two-point high-frequency injection technique is non-contact measurement of voltage in cables. From the experimental results, the impedance of the sensor can be measured and reverse-calculated as the supply voltage. The measurement accuracy of line voltage according to the test load has a percentage error of 1.5622%, 0.3097%, and 1.1591% respectively. The performance of non-contact voltage measurement is nearly compared to other techniques but is superior as far as determining the formed impedance in the sensor probe. Because the parasitic capacitance or stray capacitance can be calculated in determining the impedance of the sensor probe. Furthermore, this technique can be applied to achieve more accurate measurements by increasing the frequency points injected into the system. By injecting multiple frequencies, more calculated values per element can be obtained. And can be applied to more complex elements. Consideration of other effects on the performance of non-contact voltage measurement improves the accuracy of the non-invasive measurement system and increases its flexibility to use in various situations.

Acknowledgement

This research was not funded by any grant.

References

- [1] Shenil, P. S., and Bobby George. "An efficient digitizer for non-intrusive ac voltage measurement." In *2017 IEEE International Instrumentation and Measurement Technology Conference (I2MTC)*, pp. 1-6. IEEE, 2017. <https://doi.org/10.1109/I2MTC.2017.7969807>

- [2] Li, Songnong, Wenxin Peng, Qiang Zhou, and Xingzhe Hou. "Research on Non-contact Voltage Measurement Technology Based on Near Field Detection." In *2019 IEEE Sustainable Power and Energy Conference (ISPEC)*, pp. 2704-2707. IEEE, 2019. <https://doi.org/10.1109/ISPEC48194.2019.8974904>
- [3] Chen, Yung-Chang, Wei-Hung Hsu, Shih-Hsien Cheng, and Yu Ting Cheng. "A power sensor tag with interference reduction for electricity monitoring of two-wire household appliances." *IEEE transactions on industrial electronics* 61, no. 4 (2013): 2062-2070. <https://doi.org/10.1109/TIE.2013.2266089>
- [4] Ren, Sotara, Hiroshi Nakahara, Kittikhun Thongpull, Pornchai Phukpattaranont, and Kanadit Chetpattananondh. "A development of capacitive voltage sensor for non-intrusive energy meter." In *2018 15th International Conference on Electrical Engineering/Electronics, Computer, Telecommunications and Information Technology (ECTI-CON)*, pp. 776-779. IEEE, 2018. <https://doi.org/10.1109/ECTICon.2018.8620004>
- [5] Shenil, P. S., and Bobby George. "An auto-balancing scheme for non-contact ac voltage measurement." In *2018 IEEE 9th International Workshop on Applied Measurements for Power Systems (AMPS)*, pp. 1-5. IEEE, 2018. <https://doi.org/10.1109/AMPS.2018.8494863>
- [6] Brunelli, Davide, Clemente Villani, Domenico Balsamo, and Luca Benini. "Non-invasive voltage measurement in a three-phase autonomous meter." *Microsystem technologies* 22 (2016): 1915-1926. <https://doi.org/10.1007/s00542-016-2890-7>
- [7] Villani, Clemente, Domenico Balsamo, Davide Brunelli, and Luca Benini. "Ultra-low power sensor for autonomous non-invasive voltage measurement in IoT solutions for energy efficiency." In *Smart Sensors, Actuators, and MEMS VII; and Cyber Physical Systems*, vol. 9517, pp. 651-661. SPIE, 2015. <https://doi.org/10.1117/12.2181332>
- [8] Noppawit, Longseng, and Thongpull Kittikhun. "An Investigation of Parasitic Capacitance Determination Using High Frequency Injection Technique for Non-Contact Voltage Measurement System." In *Proceedings of Asia Pacific Conference on Robot IoT System Development and Platform*, vol. 2021, pp. 96-97. 2022.
- [9] Shenil, P. S., R. Arjun, and Bobby George. "Feasibility study of a non-contact AC voltage measurement system." In *2015 IEEE International Instrumentation and Measurement Technology Conference (I2MTC) Proceedings*, pp. 399-404. IEEE, 2015. <https://doi.org/10.1109/I2MTC.2015.7151301>
- [10] Shenil, P. S., and Bobby George. "Evaluation of a digitizer designed to interface a non-intrusive AC voltage measurement probe." *IEEE Sensors Journal* 20, no. 10 (2020): 5606-5614. <https://doi.org/10.1109/JSEN.2020.2971547>
- [11] Shenil, P. S., and Bobby George. "Nonintrusive ac voltage measurement unit utilizing the capacitive coupling to the power system ground." *IEEE Transactions on Instrumentation and Measurement* 70 (2020): 1-8. <https://doi.org/10.1109/TIM.2020.3044757>
- [12] Shenil, P. S., and Bobby George. "Development of a nonintrusive true-RMS AC voltage measurement probe." *IEEE Transactions on Instrumentation and Measurement* 68, no. 10 (2019): 3899-3906. <https://doi.org/10.1109/TIM.2019.2916959>
- [13] Lawrence, David, John S. Donnal, Steven Leeb, and Yiou He. "Non-contact measurement of line voltage." *IEEE Sensors Journal* 16, no. 24 (2016): 8990-8997. <https://doi.org/10.1109/JSEN.2016.2619666>
- [14] Thomas, Ajith John, C. Iyyappan, and C. Chakradhar Reddy. "A method for surface voltage measurement of an overhead insulated conductor." *IEEE Transactions on Instrumentation and Measurement* 70 (2020): 1-8. <https://doi.org/10.1109/TIM.2020.3021803>
- [15] Haberman, Marcelo A., and Enrique M. Spinelli. "A noncontact voltage measurement system for power-line voltage waveforms." *IEEE Transactions on Instrumentation and Measurement* 69, no. 6 (2019): 2790-2797. <https://doi.org/10.1109/TIM.2019.2926877>
- [16] Xing, Yankai, Jinpu Liu, Fuchao Li, Guangdou Zhang, and Jian Li. "Advanced dual-probes non-contact voltage measurement approach for AC/DC power transmission wire based on the electric field radiation principle." *IEEE Transactions on Instrumentation and Measurement* (2023). <https://doi.org/10.1109/TIM.2023.3315402>
- [17] Reza, Masum, and Hafiz Abdur Rahman. "Non-Invasive Voltage Measurement Technique for Low Voltage AC Lines." In *2021 IEEE 4th International Conference on Electronics Technology (ICET)*, pp. 143-148. IEEE, 2021. <https://doi.org/10.1109/ICET51757.2021.9450978>
- [18] Zhang, Xuemin, Bin Yue, Jian Huang, Yuchuan Ruan, and Peng Zhang. "Research on non-contact voltage measurement technology." In *2019 IEEE 2nd International Conference on Automation, Electronics and Electrical Engineering (AUTEEE)*, pp. 534-537. IEEE, 2019. <https://doi.org/10.1109/AUTEEE48671.2019.9033249>
- [19] Zhu, Ke, Wing Kin Lee, and Philip WT Pong. "Non-contact capacitive-coupling-based and magnetic-field-sensing-assisted technique for monitoring voltage of overhead power transmission lines." *IEEE sensors journal* 17, no. 4 (2016): 1069-1083. <https://doi.org/10.1109/JSEN.2016.2636862>
- [20] Xiao, Dongping, Yutong Xie, Qichao Ma, Qi Zheng, and Zhanlong Zhang. "Non-contact voltage measurement of three-phase overhead transmission line based on electric field inverse calculation." *IET Generation, Transmission & Distribution* 12, no. 12 (2018): 2952-2957. <https://doi.org/10.1049/iet-gtd.2017.1849>

- [21] Zheng, Wenzhe, Jian He, and Lin Zhao. "Overvoltage measurement method based on non-contact wireless measurement." In *2020 IEEE 1st China International Youth Conference on Electrical Engineering (CIYCEE)*, pp. 1-6. IEEE, 2020. <https://doi.org/10.1109/CIYCEE49808.2020.9332661>
- [22] Teverovsky, Alexander. "Effect of moisture on characteristics of surface mount solid tantalum capacitors." In *Carts-Conference-*, Pp. 96-111. Components Technology Institute Inc., 2003.